Submitted to Metallurgical Transactions

LBL-2573
Preprint c.2

STRUCTURE AND ELEVATED TEMPERATURE PROPERTIES OF CARBON-FREE FERRITIC ALLOYS STRENGTHENED BY A LAVES PHASE

RECEIVED
LAWRENCE
RADIATION LABORATORY

MAR 6 1975

LIBRARY AND
DOCUMENTS SECTION

M. Dilip Bhandarkar, M. Shanthidas Bhat,
Victor F. Zackay, and Earl R. Parker

August 1974

Prepared for the U. S. Atomic Energy Commission
under Contract W-7405-ENG-48

TWO-WEEK LOAN COPY

This is a Library Circulating Copy which may be borrowed for two weeks. For a personal retention copy, call Tech. Info. Division, Ext. 5545

LAWRENCE BERKELEY LABORATORY
UNIVERSITY OF CALIFORNIA
BERKELEY

LBL-2573
c.2

DISCLAIMER

This document was prepared as an account of work sponsored by the United States Government. While this document is believed to contain correct information, neither the United States Government nor any agency thereof, nor the Regents of the University of California, nor any of their employees, makes any warranty, express or implied, or assumes any legal responsibility for the accuracy, completeness, or usefulness of any information, apparatus, product, or process disclosed, or represents that its use would not infringe privately owned rights. Reference herein to any specific commercial product, process, or service by its trade name, trademark, manufacturer, or otherwise, does not necessarily constitute or imply its endorsement, recommendation, or favoring by the United States Government or any agency thereof, or the Regents of the University of California. The views and opinions of authors expressed herein do not necessarily state or reflect those of the United States Government or any agency thereof or the Regents of the University of California.

STRUCTURE AND ELEVATED TEMPERATURE PROPERTIES OF CARBON-FREE FERRITIC ALLOYS STRENGTHENED BY A LAVES PHASE

M. Dilip Bhandarkar, M. Shanthidas Bhat, Victor F. Zackay and Earl R. Parker

ABSTRACT

A Laves phase, Fe_2Ta, was utilized to obtain good elevated temperature properties in a carbon-free iron alloy containing 1 at. pct Ta and 7 at. pct Cr. Room temperature embrittlement resulting from the precipitation of the Laves phase at grain boundaries was overcome by spheroidizing the precipitate. This was accomplished by thermally cycling the alloys through the $\alpha \rightarrow \gamma$ transformation. The short-time yield strength of the alloys decreased very slowly with increase in test temperature up to 600°C, but above this temperature, the strength decreased rapidly. Results of constant load creep and stress rupture tests conducted at several temperatures and stresses indicated that the rupture and creep strengths of spheroidized 1Ta-7Cr alloy were higher than those of several commercial steels containing chromium and/or molybdenum carbides but lower than those of steels containing substantial amounts of tungsten and vanadium. When molybdenum was added to the base Fe-Ta-Cr alloy, the rupture and creep strengths were considerably increased.

M. Dilip Bhandarkar, formerly Post-doctoral Research Metallurgist, Lawrence Berkeley Laboratory, Berkeley, California 94720, is presently at Materials Research Branch, Materials Division, NASA Langley Research Center, Hampton, Virginia 23665; M. Shanthidas Bhat is Graduate Student, Victor F. Zackay and Earl R. Parker are Professors of Metallurgy, University of California, Berkeley, California 94720.

INTRODUCTION

Most commercially available creep resistant materials derive their strength from a uniform dispersion of a second phase which hinders the movement of dislocations. In creep resistant ferritic steels, the dispersion almost invariably consists of one or more types of carbides, whereas in high nickel content superalloys, a large volume fraction of the intermetallic compound $Ni_3(Al,Ti)$ is involved.

The composition, morphology, and crystal structure of carbides tend to change slowly at elevated temperatures, and this often results in an increase in creep rate. One example of this is found in the case of 0.1C-1Cr-0.5Mo steel. The commonly used heat treatment for this steel results in a dispersion of M_3C type carbide. On long time exposure at an elevated temperature, the carbides M_7C_3 and Mo_2C gradually form, and eventually M_6C appears. These changes are accompanied by decrease in creep resistance(1).

Another problem that is frequently encountered in elevated temperature steels arises from their need for oxidation resistance. Chromium additions are usually employed for this purpose. In steels, increasing chromium additions favor the formation of M_7C_3 and $M_{23}C_6$ type carbides(2). Neither of these carbides imparts appreciable strengthening at elevated temperatures(2-4). Colbeck and Rait(2) found a continuous decrease in the creep strength of chromium-vanadium steels as the chromium content was increased from 1 to 8 pct. On the other hand, worthwhile improvements in oxidation resistance at 600°C are not obtained in ferritic steels until about 7 pct chromium is present(3,4). Such alloys,

therefore, have inherently low creep strength due to the presence of the carbide M_7C_3. It seems desirable to eliminate carbides as the strengthening agent in creep resistant steels and to devise alternative means of enhancing elevated temperature creep strength. The use of stable intermetallic compounds is an obvious possibility. Several are known to provide significant strengthening when dispersed in iron(5).

Using intermetallic compounds rather than carbides for enhancing elevated temperature strength is a concept that is decades old, but progress towards its realization has been slow. A major deterrent has been the tendency of such compounds to precipitate at grain boundaries which leads to severe room temperature embrittlement. The effects of intermetallic compounds such as the sigma phase have been reported by Decker and Floreen(5), Decker(6), and Mihalisin et al(7). There is general agreement that the presence of the sigma phase lowers both rupture strength and room temperature ductility. Decker(6) also summarized the status of knowledge about the effects of the Laves phase in superalloys. He concluded that in general, when the Laves phase is present in significant amounts, it ".....can degrade room temperature ductility with little effect on creep properties". A similar conclusion has been reached about the effect of the Laves phase in ferritic alloys(8).

One objective of the present investigation was to obtain good room temperature ductility and elevated temperature creep strength in iron-base alloys strengthened by a Laves phase. Fe-Ta-Cr and Fe-Ta-Cr-Mo alloys were used in the present investigation. The $\alpha \rightarrow \gamma$ and $\gamma \rightarrow \delta$

transformations and microstructures were studied. Short-time tensile as well as creep and stress rupture tests were conducted on the alloys. The microstructures were varied by controlling the heat treating procedure. The mechanical properties were compared with published values of several commercially available steels.

EXPERIMENTAL PROCEDURE

High purity materials were used for making the alloys. Heats of approximately 20 lbs (9 Kg) were induction melted in an argon atmosphere, cast in heavy copper molds, and subsequently annealed in vacuum for three days at 1100°C. The nominal compositions of the alloys and designations are listed in Table I. The ingots were forged at 1100°C into 9/16 in. (14 mm) thick plates for creep specimen blanks. For tensile specimen blanks, the plates were further reduced by rolling at 1000°C to a thickness of 7/32 in. (5.6 mm). The heat treatments used and their designations are listed in Table II.

Tensile tests were performed in argon at temperatures ranging from 22° to 700°C using pin loaded sheet specimens of 1 in. (25.4 mm) gage length and a thickness of 0.2 in. (5.1 mm). The strain rate was 0.04 per min. Yield strengths were obtained by the 0.2 pct offset method. Constant load creep and stress rupture tests were carried out on cylindrical specimens with 1/2 in. (12.7 mm) diameter threaded ends and a gage section diameter of 0.25 in. (6.4 mm). A conventional extensometer fitted with dial gages was used for measurement of extension.

Metallographic and x-ray specimens were prepared by conventional

means. Thin foils and carbon replicas extracted from metallographically polished and etched specimens were used for transmission electron microscopy. Fracture surfaces were examined in a scanning electron microscope.

ALLOY SELECTION AND TREATMENTS

The Fe-Ta System

An examination of the iron-rich portion of the Fe-Ta binary phase diagram (9) indicates that three solid solutions of tantalum in iron exist in different temperature ranges, the low temperature bcc α phase, the intermediate temperature fcc γ phase, and the high temperature bcc δ phase. The maximum solid solubility of tantalum in iron occurs in the δ phase field and is 2.8 at. pct at 1440(±2)°C. The δ phase decomposes eutectoidally at 1239(±3)°C by the reaction,

$$\delta(1.1 \text{ at. pct Ta}) \rightarrow \gamma(0.5 \text{ at. pct Ta}) + Fe_2Ta$$

The γ phase reacts peritectoidally with Fe_2Ta at 972(±3)°C by the reaction,

$$\gamma(0.3 \text{ at. pct Ta}) + Fe_2Ta \rightarrow \alpha(0.6 \text{ at. pct Ta})$$

The solubility of tantalum in α iron decreases with a decrease in temperature from 972°C but the shape of the solvus curve has not been established. The compound Fe_2Ta is a Laves phase with a melting point of 1775°C(10,11). It has been suggested that the Fe-Ta Laves phase may be stable over a range of compositions somewhat similar to the Laves phase in the Fe-Nb system(12-15).

Precipitation of the Laves Phase

The results of extensive investigations of the precipitation of the Laves phase in Fe-Ta alloys with tantalum contents ranging from 0.5 to 2.5 at. pct were reported by Jones and associates(14,15). Their alloys

were solution treated at 1400°C for one hour and water quenched prior to aging at 600°C, 700°C and 800°C. An almost continuous grain boundary network of precipitate was present in the solution treated condition. Precipitation occurred in the grains during aging. The aged alloys were extremely brittle because of the large grain size and the grain boundary precipitate network(15, 16).

Enhancement of Ductility

It was found in an earlier investigation(16) that the Laves phase could be spheroidized by heat treating the alloys in the (γ + Fe_2Ta) phase field (this heat treatment is referred to as the spheroidizing treatment). When the alloys were cooled to room temperature, the resulting microstructure consisted of a uniform dispersion of almost spherical particles of Fe_2Ta in a matrix of the α solid solution. The room temperature elongation of Fe-Ta alloys increased from near zero in the aged condition to 22-30 pct after spheroidizing. A room temperature yeild strength of 40,800 psi (281 MN/m^2) was observed for the Fe-1 at. pct Ta alloy spheroidized for 10 min at 1100°C following aging for one hour at 700°C. Elevated temperature tensile tests indicated that a large fraction of the room temperature yeild strength was retained up to a test temperature of about 600°C. Above this temperature, the yield strength dropped rapidly(16).

Fe-Ta-Cr and Fe-Ta-Cr-Mo Alloys

Two major limitations of Fe-Ta alloys were: 1) the high phase transformation temperatures that necessitated high temperature heat treatments, and 2) inadequate oxidation resistance at creep temperature

(at 700°C in air, the weight gain of the Fe-1Ta alloy was about 30 pct of that of pure iron(17)). The effect of chrominum additions was explored next. Chromium additions to iron (below 7 pct) lower both the $\delta \rightarrow \gamma$ and $\gamma \rightarrow \alpha$ phase transformations(18). The oxidation of Fe-Cr alloys at 1000°C decreases significantly with chromium additions of up to about 7 pct and then remains approximately constant up to 12 pct Cr(19).

The factors discussed above led to the development of ternary Fe-Ta-Cr alloys Ta5Cr (Fe, 1 at. pct Ta, 5 at. pct Cr) and Ta7Cr (Fe, 1 at. pct Ta, 7 at. pct Cr). In both alloys, the tantalum content was limited to 1 at. pct because higher and lower tantalum contents would raise the temperatures needed to attain single phase δ during the solution heat treatment. The chromium additions served the intended purposes. To obtain further improvements in creep properties, the Fe-Ta-Cr alloys were modified by the addition of 0.5 at. pct molybdenum which is well known to be an effective high temperature strengthener.

RESULTS AND DISCUSSION

Phase Transformations and Microstructures of Fe-Ta-Cr Alloys

The temperature to attain single phase δ was lowered by 60°C with addition of 5 at. pct Cr to the Fe-1 at. pct Ta alloy, and by 90°C with addition of 7 at. pct Cr. A more detailed study of the effect of chromium additions is discussed elsewhere(20). One hour solution treatments at 1320°C were employed for both Ta5Cr and Ta7Cr alloys. The specimens were quenched in 70°C water. The microstructures were characterized by large grains (approximately 1 mm in average diameter) and an almost continuous

grain boundary film of precipitate. When the alloys were aged at an elevated temperature (e.g. 700°C), precipitation occurred within the grains, but there was no noticeable change in the grain boundary network. The alloys exhibited hardness variations with aging time similar to those reported for Fe-Ta(14). The time at 700°C to attain peak hardness was 40 min for both alloys Ta5Cr and Ta7Cr. The microstructure of the Ta7Cr alloy in the peak hardness condition is shown in Fig. 1.

In Fig. 2 is shown the transmission electron micrograph of a carbon extraction replica from a peak aged specimen of alloy Ta7Cr. The precipitate particles were mostly angular and rod shaped. Transmission electron microscopy of thin foils of alloy Ta7CrMo showed that the precipitate first formed coherently, then lost its coherency by the formation of ⟨100⟩ type dislocation loops, which in turn acted as sites for preferred nucleation and growth of precipitates during subsequent aging(21). An additional result was the observation of a relatively low density of mobile dislocations in aged alloys.

In discussions that follow, the precipitate in the alloys of the current investigation is referred to as the Laves phase, Fe_2Ta, although x-ray diffractometer studies made on specimens of alloy Ta7Cr, aged for 40 h at 700°C, indicated that the interplanar spacings of the precipitate were very nearly those reported for Fe_7Ta_3.

When the aged alloys were heated 10 min at 1100°C, the matrix transformed to the fcc solid solution γ , and both the grain boundary precipitate and the precipitate within the grains spheroidized. Optical micrographs of alloy Ta7Cr cooled from the spheroidizing treatment revealed irregular grain boundaries.

Transmission electron microscopy of thin foils of the spheroidized alloy, indicated a lath-like structure within the grains(22). Both the irregular grain structure and the lath-like structure were similar to those observed in several low carbon and non-carbon-containing iron-base alloys which undergo a massive transformation from austenite to ferrite(23,24). The substructure within the laths was characterized by a high density of dislocation tangles and subgrains. A uniform distribution of Laves phase particles of diameters 0.03-0.3 μm was observed in the spheroidized alloy, as illustrated in Fig. 3 by the transmission electron micrograph of a carbon replica.

Short-Time Tensile Properties of Fe-Ta-Cr Alloys

The short-time yeild strength of alloy Ta7Cr is plotted in Fig. 4 as a function of test temperature for both the aged (Heat Treatment T-0) and the spheroidized (Heat Treatment T-1) conditions. The yield strength decreased as the test temperature increased. Decrease in strength was gradual up to a test temperature of about 600°C; at this temperature the yield strength of the aged alloy was about 70 pct of the room temperature value. When the test temperature was raised further, the yield strength decreased more rapidly. The higher strength levels of the spheroidized alloy were attributed mainly to its higher dislocation density. A refinement of the grain size (from about 1 mm in the aged condition to about 200 μm in the spheroidized condition) due to the $\alpha \rightarrow \gamma \rightarrow \alpha$ phase change cycle that accompanied the spheroidizing treatment was also a possible factor contributing to the higher strength.

Scanning electron fractographs of tensile specimens of the alloy Ta7Cr, aged at 700°C for 40 min, tested at various temperatures are

shown in Fig. 5. The fracture surface of the specimen tested at 22°C (Fig. 5(a)) was characterized by flat areas, steps, and river markings which are typical cleavage features. Fracture was apparently initiated at the grain boundary precipitate envelope and propagated in a transgranular manner. Fracture surfaces of specimens tested at 200°C (Fig. 5(b)), 400°C (Fig. 5(c)), and 600°C (Fig. 5(d)) indicated increasingly ductile behavior, and fracture was characterized by cleavage, quasi-cleavage, and ductile tearing at 200°C, quasi-cleavage, ductile tearing, and dimpled rupture at 400°C, and predominantly dimpled rupture at 600°C. A large portion of the dimpled rupture observed at 600°C was initiated by void formation at precipitate-matrix interfaces (Fig. 5(d)). Figure 5(d) also shows dimples formed by extensive ductile tearing. Void formation and ductile tearing resulted in a fracture appearance characterized by wide range of dimple sizes.

The scanning electron fractograph of the tensile specimen of alloy Ta7Cr spheroidized at 1100°C for 10 min (Heat Treatment T-1), and tested at 22°C exhibited dimpled rupture, Fig. 6. Dimple formation was almost entirely initiated by void formation at precipitate-matrix interfaces. Typically there were large dimples of sizes ranging from 10 to 25 μm separated by areas with smaller dimples of sizes 1 μm or less. Precipitate particles as large as 4 μm were observed in the larger dimples. Similar large particles were also observed on fracture surfaces of creep specimens. Void formation was initiated apparently at these large precipitate particles, and plastic flow resulted in the growth of the voids to a stage when final fracture resulted by failure of the areas between

the large voids. The room temperature fracture elongation increased from 13 pct to 20 pct as a result of the spheroidizing treatment. The increase in room temperature fracture elongation and the change in fracture morphology from brittle in the aged alloy to ductile in the spheroidized alloy were attributed to the change in precipitate morphology and distribution resulting from the spheroidizing treatment.

Variations in spheroidizing treatment, involving cold working and repeated thermal cycling, resulted in microstructural changes, but did not significantly affect elevated temperature yield strength of alloy Ta7Cr. In Fig. 7 the short-time yield strength is plotted vs test temperature for the heat treatments T-1, T-2, T-3, T-4 and T-5 described in Table II. The yield strength data for T-1, T-2, T-3 and T-4 were within a narrow band which decreased in width for increasing test temperature above 500°C. Cold working the spheroidized alloy at room temperature to a 20 pct reduction in thickness (Heat Treatment T-5) led to a 40 pct increase in room temperature yield strength, but the high dislocation density resulting from the cold work was less effective in enhancing elevated temperature yield strength. At 700°C the aged alloy and the alloy with spheroidizing treatments T-1, T-2, T-3, T-4 and T-5 exhibited the same yield strength although their microstructures were considerably different. As indicated later and discussed elsewhere(21), creep and stress rupture properties were strongly influenced by microstructure.

Stress Rupture Properties of Alloys Ta7Cr and Ta7CrMo

Constant load stress rupture tests were conducted at temperatures from 900°F (483°C) to 1200°F (649°C) on spheroidized alloys Ta7Cr (Heat

Treatment T-1) and Ta7CrMo (Heat Treatments T-2A and T-6). Plots of stress vs rupture time at 1000°F (538°C) are shown in Fig. 8 for alloy Ta7Cr and several commercial ferritic steels(25). It was observed that at 1000°F (538°C) the rupture strength of alloy Ta7Cr was lower than those of 0.3C-1Cr-1Mo-0.25V steel, type 422 stainless steel, and Greek Ascoloy, but was higher than those of 0.15C-9Cr-1Mo steel, 0.15C-7Cr-0.5Mo steel, and types 403 and 410 stainless steels. Comparison with results reported in the literature for several ferritic alloys revealed that in general, the rupture strength of alloy Ta7Cr was higher than those of steels with chromium contents between 5 and 12 pct and containing dispersions of chromium and molybdenum carbides. Rupture strength of steels containing significant volume fractions of carbides of elements such as vanadium and tungsten was much higher than that of alloy Ta7Cr.

Examination of structural features of specimens of alloy Ta7Cr before and after creep testing indicated that partial recovery of dislocation substructure occurred in the alloy. It was of interest to examine if further alloying by solid solution strengthening would enhance creep strength by retarding recovery. Molybdenum was chosen as the alloying element for this purpose, since it is well known(26-30) that molybdenum is a very effective elevated temperature strengthener in ferrite.

The addition of 0.5 at. pct Mo alloy Ta7Cr, leading to the alloy Ta7CrMo, did not alter the aging behavior but did, however, cause a considerable change in the kinetics of the $\alpha \rightarrow \gamma$ transformation. The $\alpha \rightarrow \gamma$ transformation exhibited a unique time-temperature dependence which is discussed in detail elsewhere(21). At the spheroidizing temperature of

1100°C, a 10 min hold time was not sufficient for completion of the $\alpha \rightarrow \gamma$ transformation. Two spheroidizing treatments, one involving a 2 h hold at 1100°C and the other, three repeated cycles between room temperature and 1100°C (with a 15 min hold at 1100°C during each cycle), resulted in the completion of the $\alpha \rightarrow \gamma$ phase transformation. X-ray diffractometer studies revealed that the interplanar spacings of the Laves phase precipitate that formed in alloy Ta7CrMo were approximately the same as those of the Laves phase in alloy Ta7Cr.

The elevated temperature short-time yield strengths of alloy Ta7CrMo, for the spheroidizing heat treatments of 2 h at 1100°C, and three 15 min cycles between 1100°C and room temperature (Heat Treatments T-6 and T-2A respectively in Table II) were only slightly higher than that of alloy Ta7Cr. However, the creep and rupture strengths of alloy Ta7CrMo were considerably greater than those of alloy Ta7Cr.

The plots of stress vs rupture time at 1100°F (593°C) are shown in Fig. 9 for alloy Ta7CrMo heat treated according to procedures T-2A and T-6. Also shown in the figure are the results for alloy Ta7Cr (Heat Treatment T-1) and the properties reported in the literature(25) for several commercial steels. The rupture strength of alloy Ta7CrMo was strongly influenced by the heat treating procedure, as was evident from a comparison of the plots of stress vs rupture time for the Heat Treatments T-2A and T-6. Heat Treatment T-6 resulted in rupture strengths very nearly equal to, and in fact slightly higher than, the rupture strengths of Greek Ascoloy.

Creep Rates of Alloys Ta7Cr and Ta7CrMo

Steady state creep rates were determined at several stresses and temperature for alloys Ta7Cr (Heat Treatment T-1) and Ta7CrMo (Heat Treatments T-2A and T-6). The Ta7Cr alloy results at 1000°F (538°C) and 1100°F (593°C) are plotted against stress on a log-log plot in Fig. 10. A stress sensitivity of steady state creep rate of 6.5 was estimated from the figure. A similar value has been reported by Amin and Dorn(31) for a dispersion strengthened steel.

A measure of creep strength is provided by the stress required for a creep rate of 1×10^{-4} pct/h. For alloy Ta7Cr (Heat Treatment T-1), the values of the stress for a creep rate of 1×10^{-4} pct/h at 1000°F (538°C) and 1100°F (593°C) were determined from Fig. 10 by extrapolation. The 1000°F (538°C) value is compared in Table III with the values reported in the literature for several commercially available ferritic steels(25,32). It can be observed from Table III that the creep strength of alloy Ta7Cr was higher than the creep strength of 0.3C-1Cr-1Mo-0.25V, 0.15C-7Cr-0.5Mo, and 0.15C-9Cr-1Mo steels, and types 403 and 410 stainless steels, but lower than that of type 422 stainless steel.

The creep strength of alloy Ta7CrMo was superior to that of alloy Ta7Cr. At 1100°F (593°C), a stress of 15,000 psi (103.4 MN/m^2) was needed to cause a creep rate of 1×10^{-4} pct/h in alloy Ta7CrMo heat treated according to T-2A prior to testing. The result is compared in Table IV with the stress for 1×10^{-4} pct/h creep rate for alloy Ta7Cr (Heat Treatment T-1) and several commercial ferritic steels(25,32). It was evident that among the steels listed, only AISI type 422 stainless

steel has a higher creep strength than alloy Ta7CrMo. The stress for a creep rate of 1×10^{-4} pct/h at 1100°F (593°C) for alloy Ta7CrMo was raised to 26,000 psi (179.2 MN/m^2) when the alloy was heat treated according to procedure T-6. A comparison of this value with those in Table IV shows that the value was higher than that reported for AISI type 422 stainless steel.

SUMMARY AND CONCLUSIONS

A Laves phase Fe_2Ta was utilized to develop carbon-free creep resistant bcc iron alloys containing 1 at. pct Ta and 7 at. pct Cr. Precipitation of the Laves phase led to considerable hardening of Fe-Ta-Cr and Fe-Ta-Cr-Mo alloys. The room temperature embrittlement resulting from grain boundary precipitation was overcome by using an allotropic $\alpha \rightarrow \gamma$ phase transformation which resulted in spheroidization of the precipitate. The structure of a spheroidized alloy Ta7Cr, containing 1 at. pct Ta and 7 at. pct Cr, was characterized by a uniform distribution of almost spherical particles of the Fe-Ta Laves phase in a bcc matrix with irregular grain boundaries. Particle diameters of the precipitate ranged from 0.03 to 4μm. Examination by transmission electron microscopy revealed a lath-like substructure consisting of subgrains and tangled dislocation networks. A high density of unpinned dislocations was present.

Both the aged, and aged and spheroidized Fe-Ta-Cr alloys maintained considerable fractions of their room temperature strengths up to a test temperature of about 600°C. At temperatures higher than about 600°C the strength decreased sharply. Variations in heat treating procedure, involving cold working before aging, and repeated cycling between room temperature and the spheroidizing temperature, did not cause significant

changes in short-time tensile properties of alloy Ta7Cr, particularly at test temperatures in the neighborhood of 700°C. A substructure developed by cold working the spheroidized Ta7Cr alloy was not effective in enhancing short-time yield strength at temperatures higher than about 700°C.

The results of constant load creep and stress rupture tests, conducted at several stresses and temperatures on spheroidized alloy Ta7Cr, indicated that, in general, the rupture strength of the alloy was higher than that of ferritic steels containing 5 to 12 pct Cr and strengthened by dispersions of chromium and molybdenum carbides, but lower than that of ferritic steels containing significant amounts of vanadium and tungsten as solid solution strengtheners and carbide formers. The steel 0.3C-1Cr-1Mo-0.25V had higher rupture strength but lower creep strength than alloy Ta7Cr.

Solid solution alloying by addition of 0.5 at. pct molybdenum to alloy Ta7Cr resulted in significant changes in the $\alpha \rightarrow \gamma$ transformation characteristics and considerable improvement in creep and rupture strengths. The creep properties of alloy Ta7CrMo, containing 1 at. pct Ta, 7 at. pct Cr, and 0.5 at. pct Mo, were strongly influenced by microstructural changes caused by variations in heat treating procedure. Rupture strengths higher than those of Greek Ascoloy and creep strengths superior to those of type 422 stainless steel were obtained at 1100°F (593°C) for alloy Ta7CrMo.

ACKNOWLEDGMENT

This work was performed under the auspices of the United States Atomic Energy Commission through the Inorganic Materials Research Division of the Lawrence Berkeley Laboratory at the University of California.

REFERENCES

1. L. H. Toft and R. A. Marsden: Structural Processes in Creep, Iron Steel Inst. Spec. Rep. No. 70, p. 276, The Iron and Steel Institute, London, 1961.
2. E. W. Colbeck and J. R. Rait: Symposium on High Temperature Steels and Alloys for Gas Turbines, Iron Steel Inst. Rep. No. 43, p. 107,1952.
3. G. A. Mellor and S. M. Barker: J. Iron Steel Inst., 1960, vol. 194 p. 464.
4. J. H. Woodhead and A. G. Quarrell: J. Iron Steel Inst., 1965, vol. 203, p. 605.
5. R. F. Decker and S. Floreen: Precipitation from Iron-Base Alloys, G. R. Speich and J. B. Clark, eds., AIME Met. Soc. Conf. vol. 28, p. 69, Gordon and Breach Science Publishers, New York, 1965.
6. R. F. Decker: Steel Strengthening Mechanisms, p. 147, Climax Molybdenum Co., Greenwich, Connecticut, 1969.
7. J. R. Mihalisin, C. G. Bieber, and R. T. Grant: Trans. TMS-AIME, 1968, vol. 242, p. 2399.
8. M. G. Gemmill, H. Hughes, J. D. Murry, F. B. Pickering, and K. W. Andrews: J. Iron Steel Inst., 1956, vol. 184, p. 122.
9. A. K. Sinha and W. Hume-Rothery: J. Iron Steel Inst., 1967, vol. 205, p. 671.
10. H. J. Wallbaum: Z. Krist., 1941, vol. 103, p. 391.
11. M. Hansen: Constitution of Binary Alloys, 2nd ed., p. 720, McGraw-Hill Book Co., Inc., New York, 1958.

12. R. P. Elliott: Constitution of Binary Alloys, First Supplement, p. 255, McGraw-Hill Book Co., Inc., New York, 1965.

13. L. Brewer: High Strength Materials, V. F. Zackay, ed., p. 12, John Wiley and Sons, Inc., New York, 1965.

14. R. H. Jones: Ph. D. Thesis, LBL-179, University of California, Berkeley, California, October 1971.

15. R. H. Jones, V. F. Zackay, and E. R. Parker: Met. Trans., 1972, vol. 3, p. 2835

16. R. H. Jones, E. R. Parker, and V. F. Zackay: Electron Microscopy and Structure of Materials, G. Thomas and R. M. Fulrath, eds., p. 829, University of California, Berkeley, California, 1972.

17. A. Baghdasarian: University of California, Berkeley, California, unpublished research, 1971.

18. M. Hansen: Constitution of Binary Alloys, 2nd ed., p. 525, McGraw-Hill Book Co., Inc., New York, 1958.

19. Welding Handbook, Section 4, p. 643, A. L. Phillips, ed., 5th ed., American Welding Society, New York, New York, 1966.

20. S. Jin: M. S. Thesis, LBL-443, University of California, Berkeley, California, December 1971.

21. M. S. Bhat: M. S. Thesis, LBL-2277, University of California, Berkeley, California, April 1974.

22. M. D. Bhandarkar: D. Eng. Thesis, LBL-1858, University of California, Berkeley, California, September 1973.

23. J. B. Massalski: Phase Transformations, p. 433, American Society for Metals, Metals Park, Ohio, 1970.

24. V. K. Lindroos and K. O. Vilpponen: Electron Microscopy and Structure of Materials, G. Thomas and R. M. Fulrath, eds., p. 732, University of California, Berkeley, California, 1972.

25. Metals Handbook, vol. 1, American Society for Metals, Metals Park, Ohio, 1968.

26. C. R. Austin, C. R. St. John, and R. W. Lindsay: Trans. AIME, 1945, vol. 162, p. 84.

27. S. F. Reiter and W. R. Hibbard, Jr.: Trans. AIME, 1955, vol. 203, p. 655.

28. A. E. Powers: Trans. AIME, 1956, vol. 206, p. 1373.

29. E. R. Parker: Proc. ASTM, 1960, vol. 60, p. 1.

30. B. B. Argent, M. N. van Niekerk, and G. A. Redfern: J. Iron Steel Inst., 1970, vol. 208, p. 830.

31. K. E. Amin and J. E. Dorn: Acta Met., 1969, vol. 17, p. 1429.

32. F. J. Clauss: Engineers Guide to High Temperature Materials, Addison and Wesley Publishing Co., Inc., Reading, Massachusetts, 1971.

Table I. Compositions and Designations of Alloys

Alloy Designation	Compositions, At. pct			
	Ta	Cr	Mo	Fe
Ta5Cr	1	5	-	Bal
Ta7Cr	1	7	-	Bal
Ta7CrMo	1	7	0.5	Bal

TABLE II. Heat Treatments and Designations

Heat Treatment	Designation
Solution treated at 1320°C for 1 h, and aged at 700°C for 40 min.	T-0
Solution treated at 1320°C for 1 h, aged at 700°C for 40 min, and spheroidized at 1100°C for 10 min.	T-1
Solution treated at 1320°C for 1 h, aged at 700°C for 40 min, and cycled 3 times between 1100°C and 22°C. Holding time at 1100°C was 10 min each time.	T-2
Solution treated at 1320°C for 1 h, cold rolled to a 50 pct reduction in thickness at 22°C, aged at 700°C for 40 min, and spheroidized at 1100°C for 10 min.	T-3
Solution treated at 1320°C for 1 h, aged at 700°C for 2 h, and spheroidized at 1100°C for 10 min.	T-4
Heat treated as for T-1, and cold rolled at 22°C to a 20 pct reduction in thickness.	T-5
Solution treated at 1350°C for 1 h, aged at 700°C for 1 h, and cycled 3 times between 1100°C and 22°C. Holding time at 1100°C was 15 min each time.	T-2A
Solution treated at 1350°C for 1 h, aged at 700°C for 1 h, and spheroidized at 1100°C for 2 h.	T-6

Specimens were quenched in hot water (70°C) following solution treatment and air cooled following aging and spheroidizing.

TABLE. III. Stress for a Creep Rate of 1×10^{-4} pct/h at 1000°F (538°C) for Alloy Ta7Cr and Commercial Steels.

Alloy	Stress for Creep Rate of 1×10^{-4} pct/h	
	psi	MN/m^2
Ta7Cr (Heat Treatment T-1)	22,400	154.4
0.3C-1Cr-1Mo-0.25V Steel	16,700	115.1
0.15C-9Cr-1Mo Steel	12,500	86.2
0.15C-7Cr-0.5Mo Steel	8,800	60.6
403 and 410 Stainless	10,000	68.9
422 Stainless	39,000	269.0

TABLE IV. Stress for a Creep Rate of 1×10^{-4} pct/h at 1100°F (593°C) for Alloy Ta7Cr, Ta7CrMo and Commercial Steels.

Alloy	Stress for Creep Rate of 1×10^{-4} pct/h	
	psi	MN/m^2
Ta7Cr (Heat Treatment T-1)	9,400	64.8
Ta7CrMo (Heat Treatment T-2A)	15,000	103.4
0.3C-1Cr-1Mo-0.25V Steel	--*	--
0.15C-9Cr-1Mo Steel	6,300	43.4
0.15C-7Cr-0.5Mo Steel	4,000	27.6
403 and 410 Stainless	4,000	27.6
422 Stainless	19,000	131.0

*Creep strength considerably changes with time at temperature.

FIGURE CAPTIONS

Fig. 1 Optical micrograph showing the microstructure of alloy Ta7Cr solution treated at 1320°C for 1 h and aged at 700°C for 40 min.

Fig. 2 Transmission electron micrograph of a carbon replica showing the Laves phase particles extracted from alloy Ta7Cr. The alloy was solution treated at 1320°C for 1 h, and aged at 700°C for 40 min prior to extraction of precipitate.

Fig. 3 Transmission electron micrograph of a carbon replica showing the Laves phase particles extracted from alloy Ta7Cr spheroidized at 1100°C for 10 min (Heat Treatment T-1).

Fig. 4 Effect of test temperature on the short-time yield strength of alloy Ta7Cr (Heat Treatments T-0 and T-1).

Fig. 5 Scanning electron fractographs of alloy Ta7Cr (Heat Treatment T-0) tested in short-time tensile tests at (a) 22°C, (b) 200°C, (c) 400°C, and (d) 600°C.

Fig. 6 Scanning electron fractograph of alloy Ta7Cr tested in short-time tensile tests at 22°C following Heat Treatment T-1.

Fig. 7 Yield strength vs test temperature for alloy Ta7Cr heat treated by processes T-1, T-2, T-3, T-4 and T-5.

Fig. 8 Stress vs rupture time at 1000°F (538°C) for alloy Ta7Cr (Heat Treatment T-1). Also shown are the results reported in the literature(25) for 0.3C-1Cr-1Mo-0.25V steel, 0.15C-9Cr-1Mo steel, AISI types 403, 410 and 422 stainless steels, and Greek Ascoloy.

Fig. 9 Stress vs rupture time at 1100°F (593°C) for alloys Ta7Cr (Heat Treatment T-1) and Ta7CrMo (Heat Treatments T-2A and T-6). Also shown are the results reported in the literature(25) for 0.3C-1Cr-1Mo-0.25V steel, 0.15C-9Cr-1Mo steel, AISI types 403, 410 and 422 stainless steels, and Greek Ascoloy.

Fig. 10 Stress vs steady state creep rate of alloy Ta7Cr (Heat Treatment T-1), at test temperatures indicated.

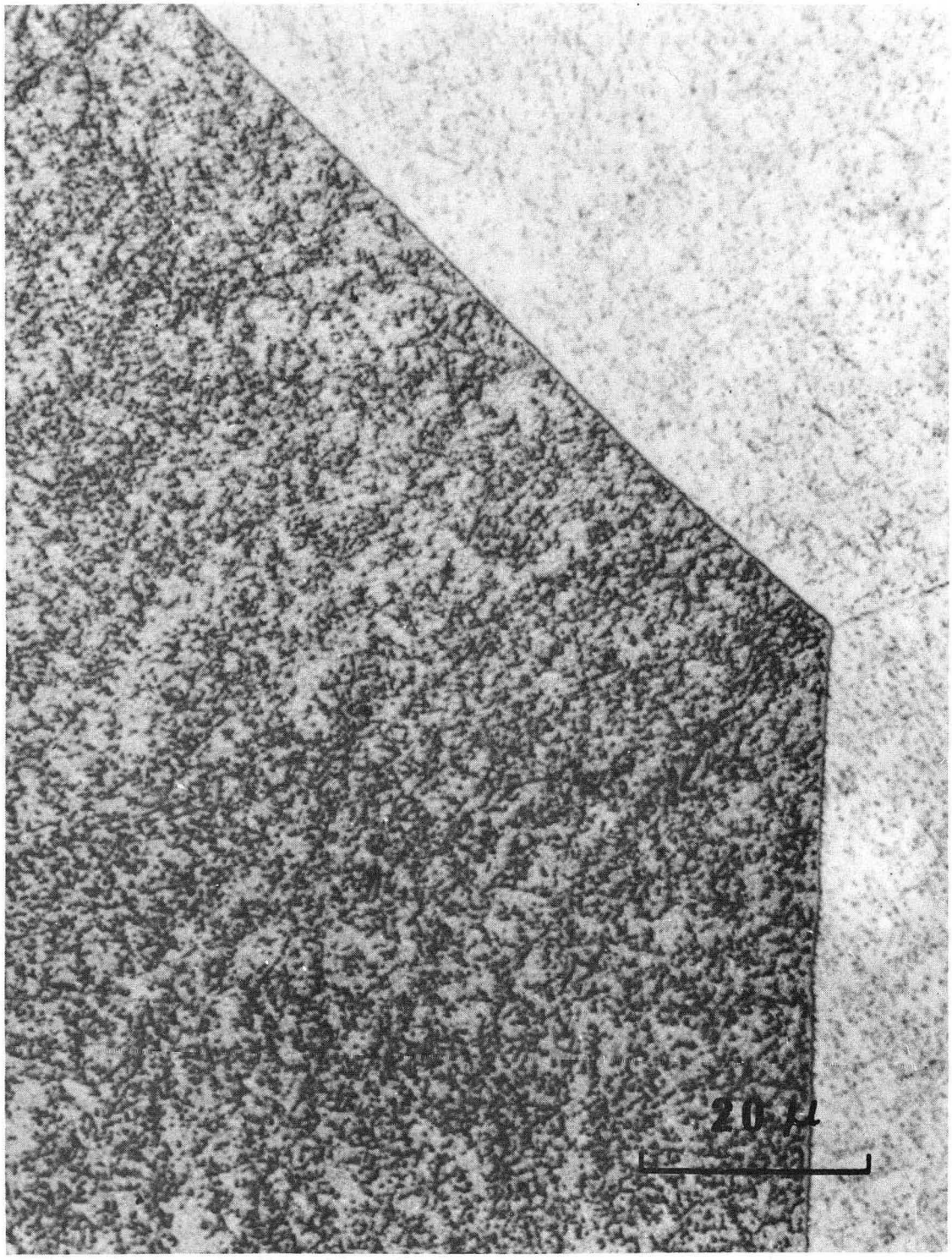

XBB 7210-4986

Fig. 1

XBB 738-5042

Fig. 2

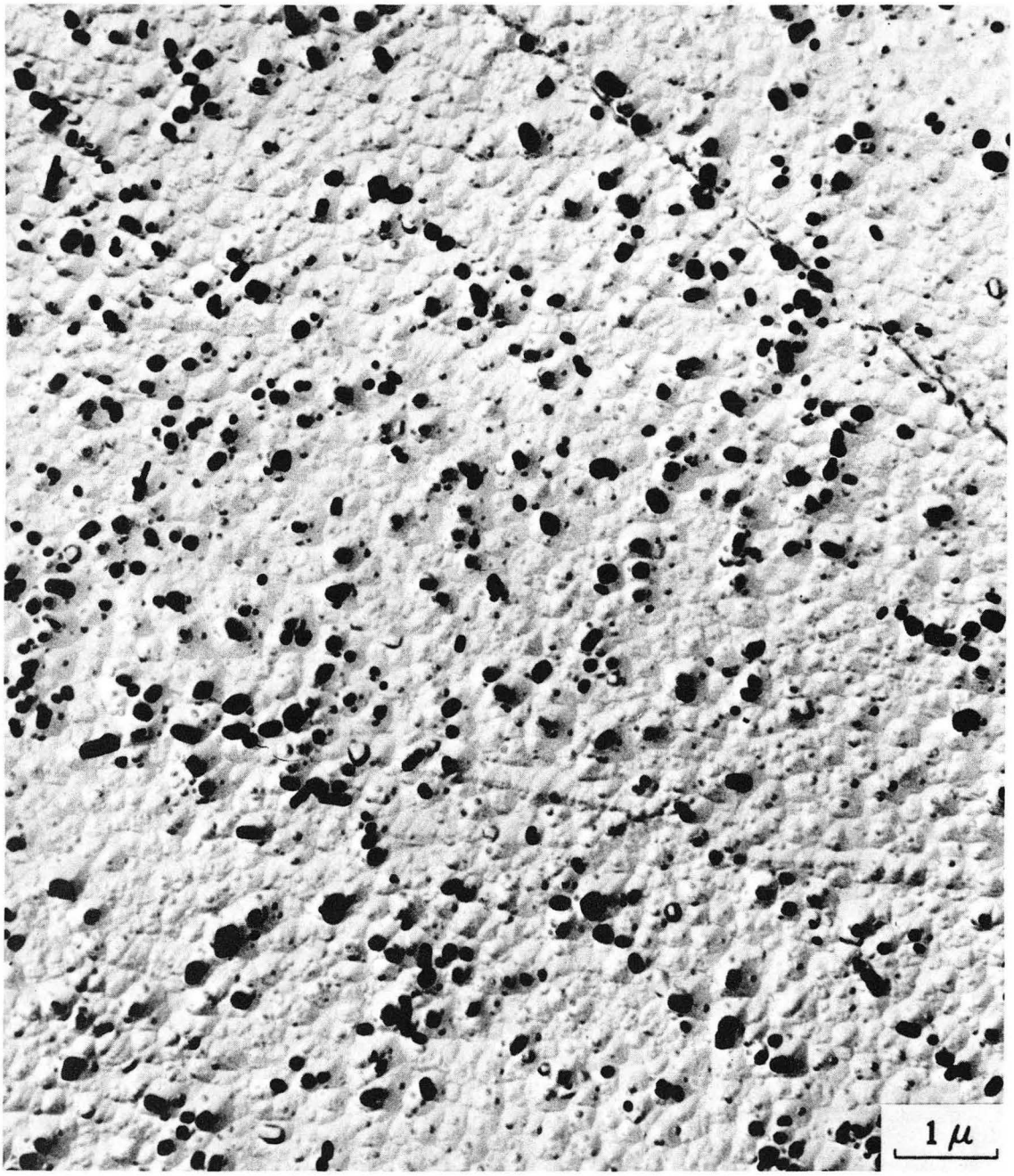

XBB 738-5043

Fig. 3

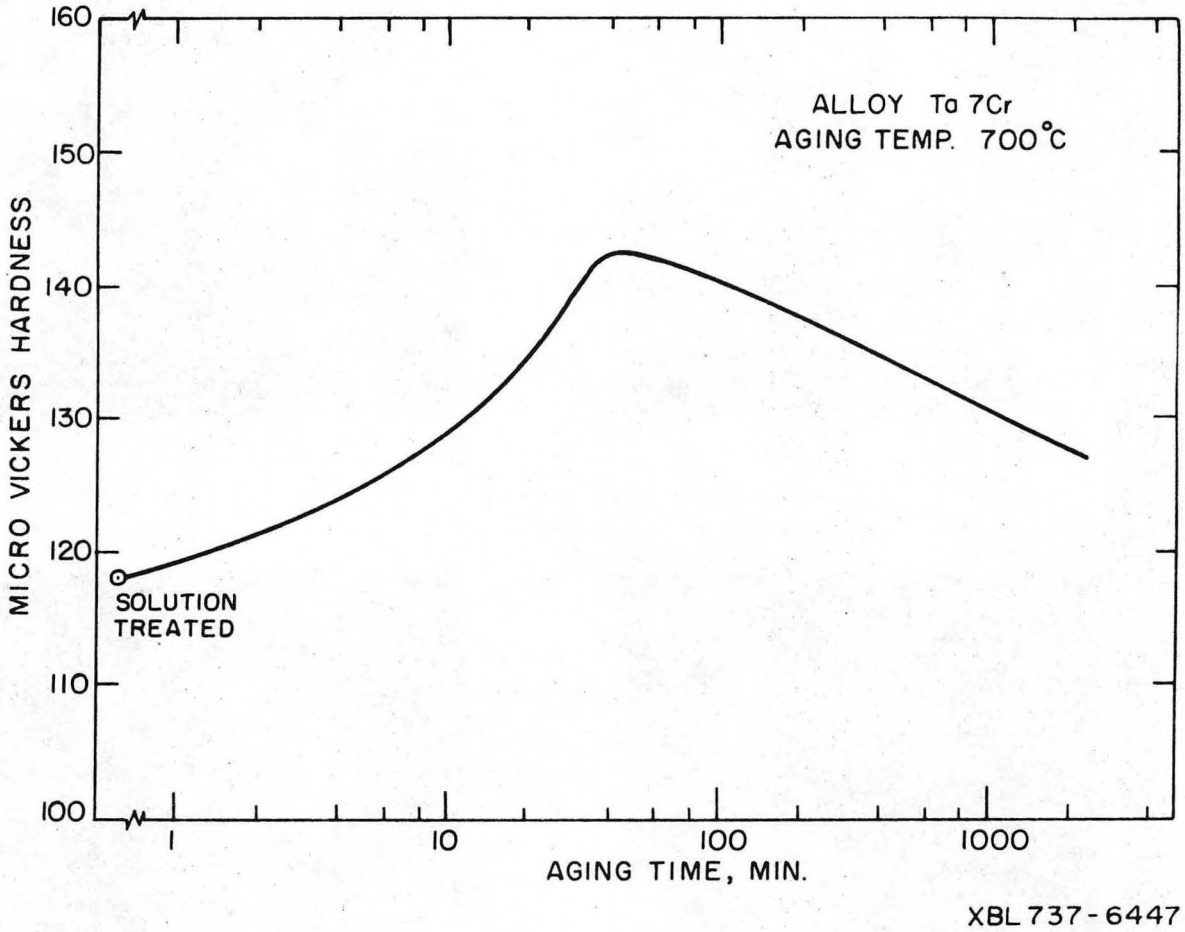
ALLOY Ta 7Cr
AGING TEMP. 700°C
MICRO VICKERS HARDNESS
160
150
140
130
120
110
100
SOLUTION
TREATED
1
10
100
1000
AGING TIME, MIN.
XBL 737-6447

Fig. 4

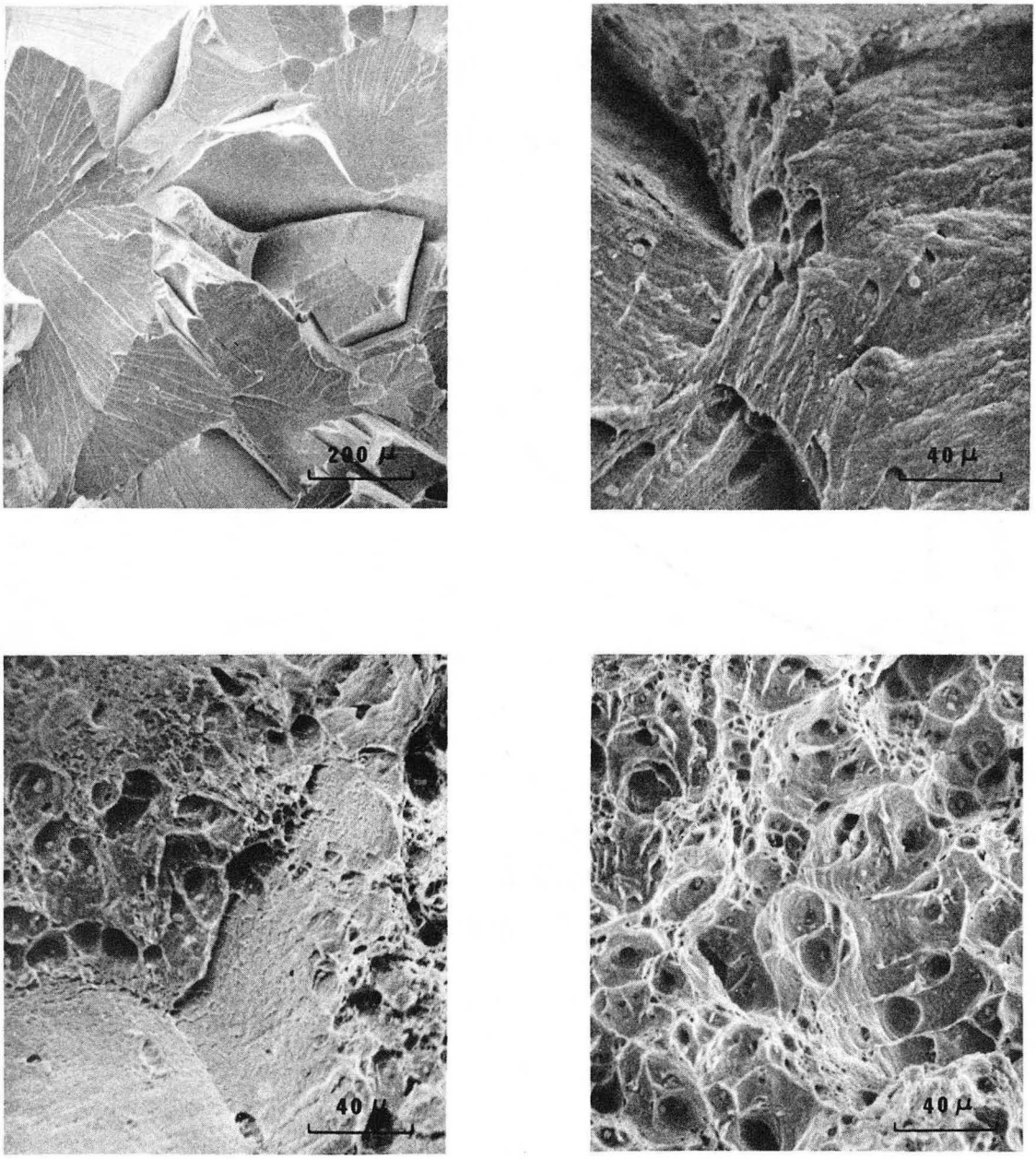

XBB 738-4992

Fig. 5

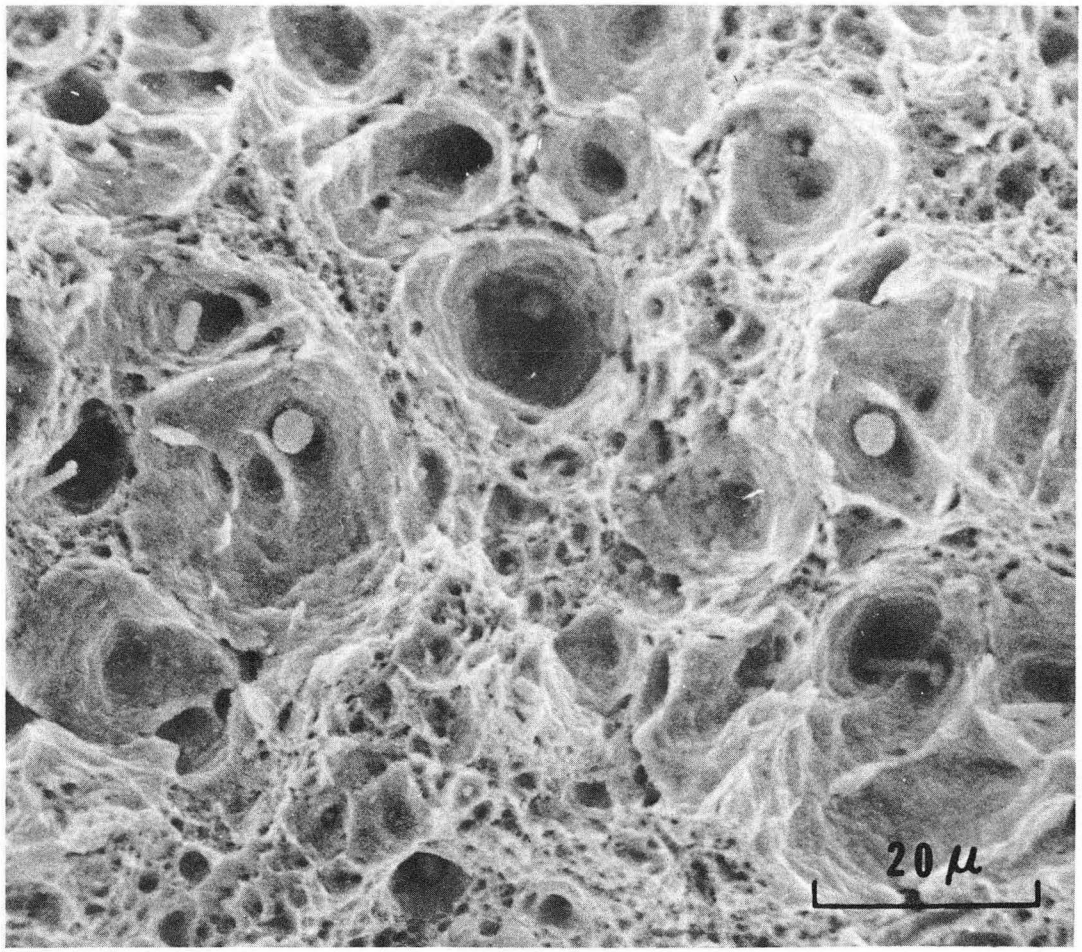

XBB 738-5037
(top)

Fig. 6

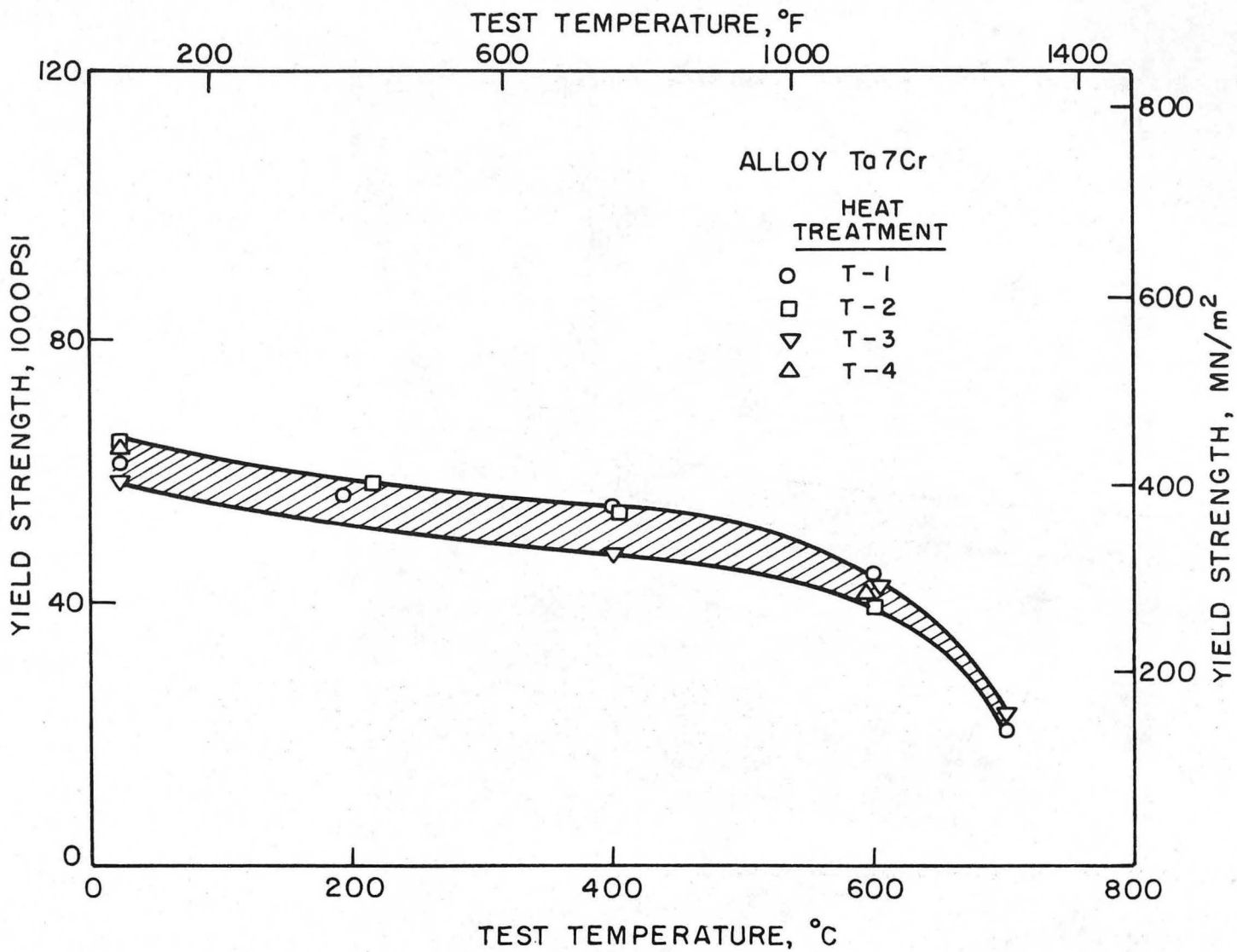

Fig. 7.

XBL737-6450A

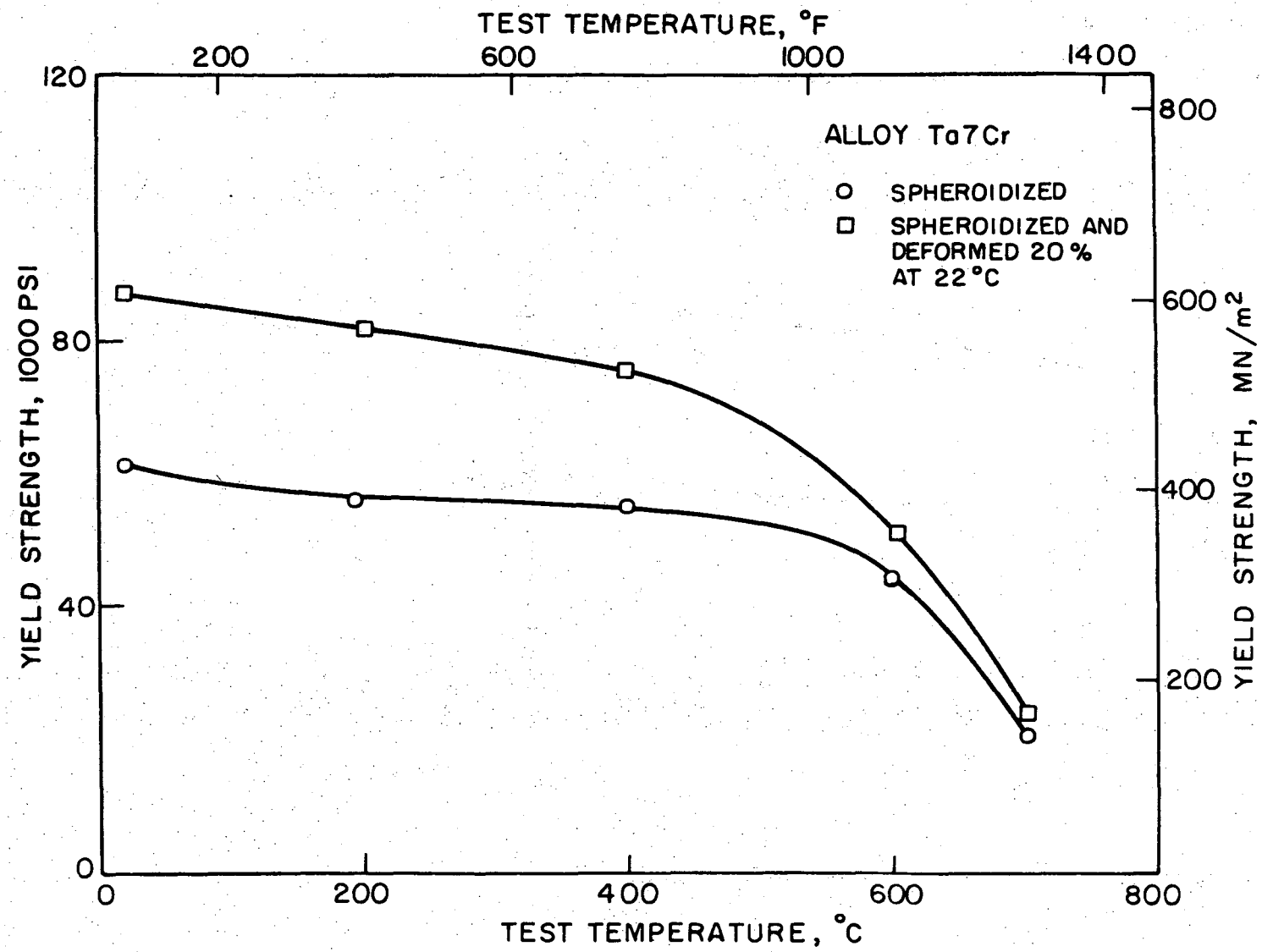

Fig. 8

XBL737-6451A

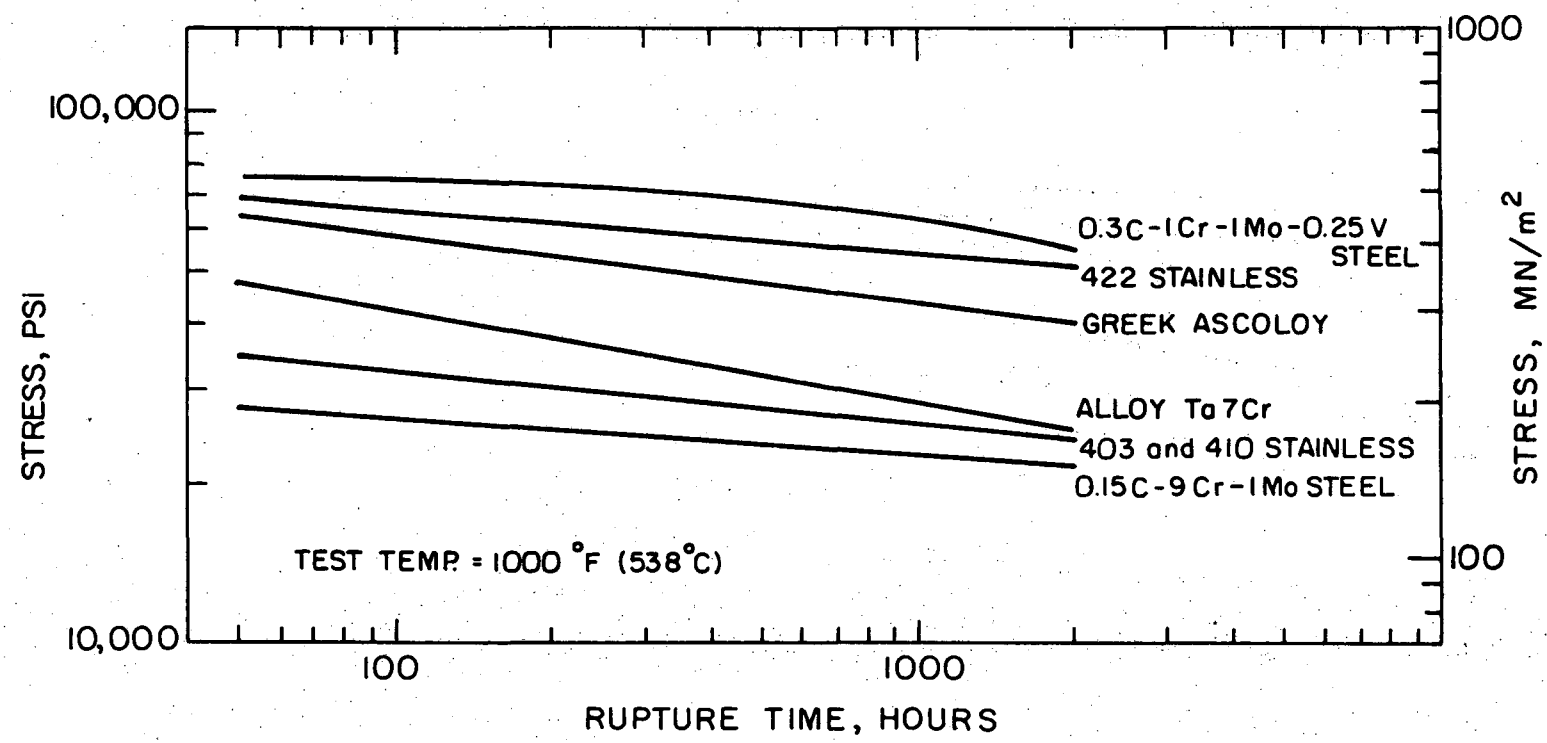

Fig. 8
(Continued)

XBL 738-1772A

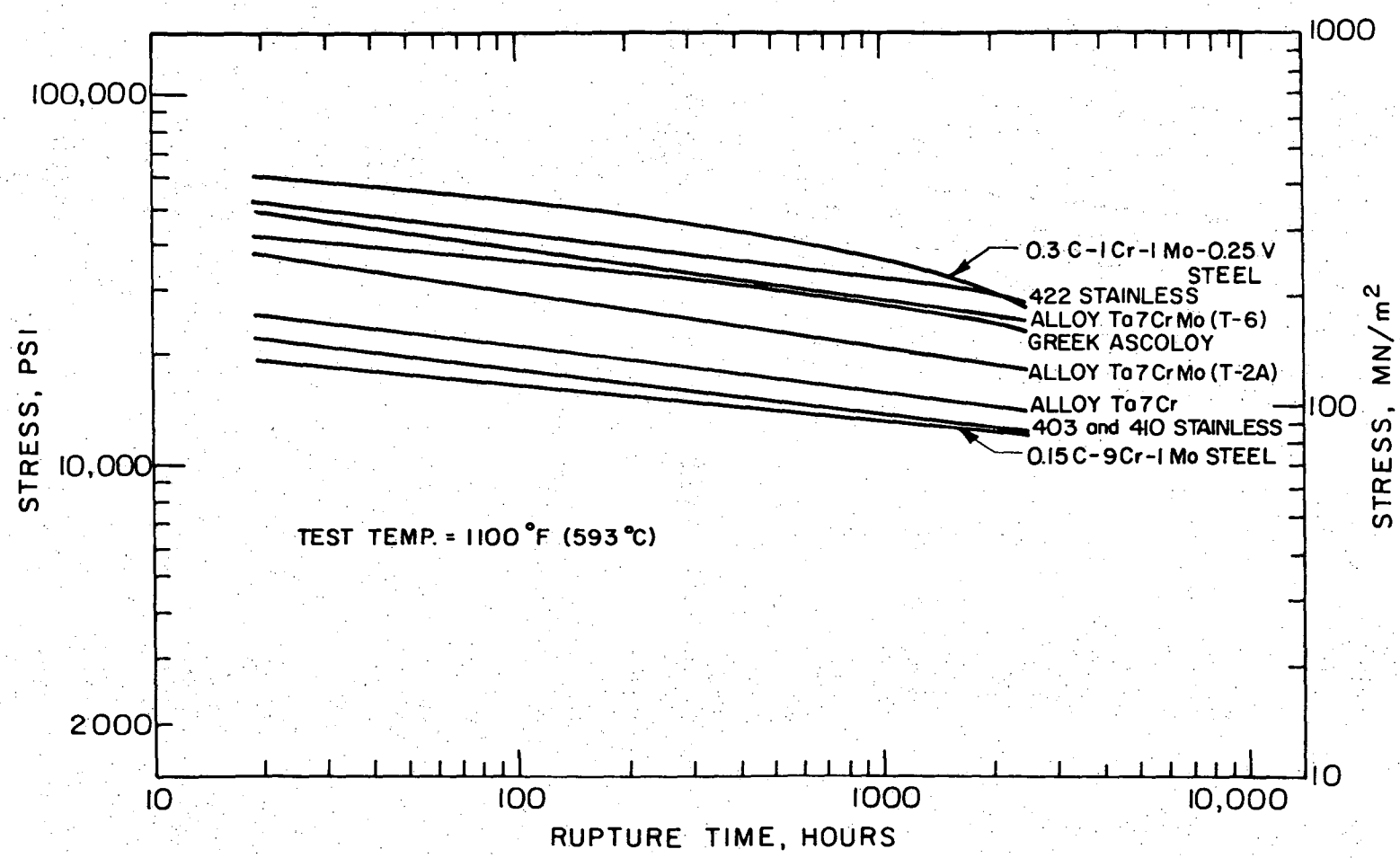

Fig. 9

XBL 745-6306

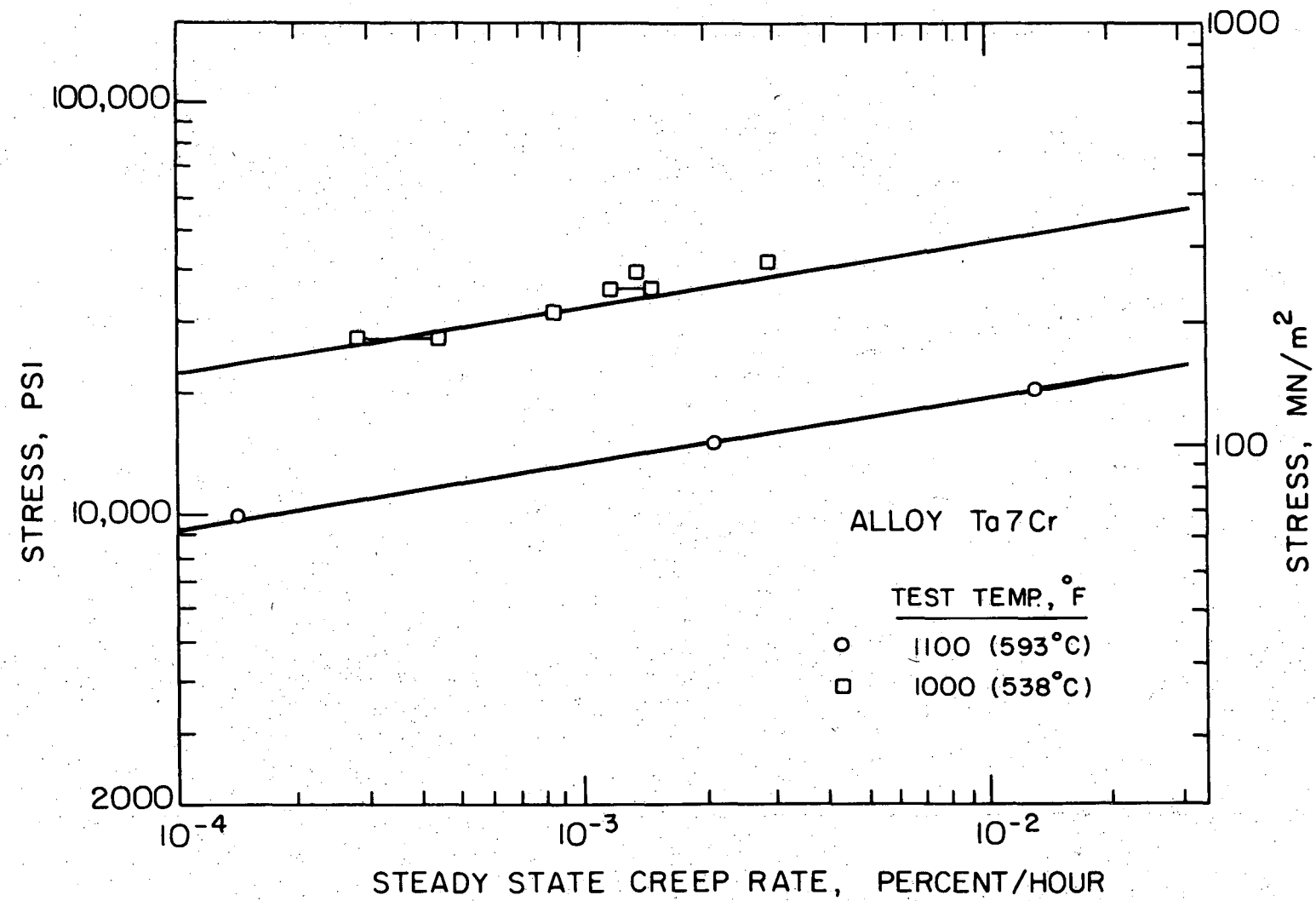

XBL738-1776A

Fig. 10

LEGAL NOTICE

This report was prepared as an account of work sponsored by the United States Government. Neither the United States nor the United States Atomic Energy Commission, nor any of their employees, nor any of their contractors, subcontractors, or their employees, makes any warranty, express or implied, or assumes any legal liability or responsibility for the accuracy, completeness or usefulness of any information, apparatus, product or process disclosed, or represents that its use would not infringe privately owned rights.

TECHNICAL INFORMATION DIVISION
LAWRENCE BERKELEY LABORATORY
UNIVERSITY OF CALIFORNIA
BERKELEY, CALIFORNIA 94720